

NEW CAPACITY AND ENERGY BASED DAMAGE INDEX

Sergio A. DÍAZ¹, Luis G. PUJADES², Alex H. BARBAT³, Yeudy F. VARGAS⁴, José R. GONZÁLEZ-DRIGO⁵, Rodrigo E. ALVA⁶

ABSTRACT

Non-linear dynamic analysis and the damage index of Park-Ang have been often used to assess expected seismic damage to a structure. Depending on the size of the structure and the duration of the record, the computational effort in dynamic analyses is usually high. In this research, a new damage index is proposed based on nonlinear static analysis. The damage index is a linear combination of two energy functions: 1) the strain energy associated with the stiffness variation and the ductility of the structure, and 2) the dissipated energy associated with hysteretic cycles. These two energy functions are obtained from the capacity curve of the structure and from the energy balance with the spectral acceleration. To show the ability of the index to represent damage, low-rise steel buildings were studied under the seismic actions that are expected in Mexico City. The results obtained with the new method show good agreement with those calculated by means of dynamic analyses using the Park-Ang damage index. On average, the Park-Ang damage index is well-fitted by the combination of 62% of the strain energy and 38% of the energy dissipated by hysteresis. Moreover, the new damage index can link damage to certain characteristics of seismic actions, such as their intensity and duration. Therefore, the new approach results in a practical, powerful tool for estimating seismic damage in buildings, especially as probabilistic approaches require massive computations.

Keywords: capacity curve; damage assessment; strain energy; energy dissipated by hysteresis; Monte Carlo simulations.

1. INTRODUCTION

In assessments of the seismic performance of buildings, the incremental dynamic analysis (IDA) (Vamvatsikos and Cornell 2002) has proved to be the most realistic, suitable, sophisticated, numerical tool to estimate the seismic response as a function of the earthquakes intensity. The IDA can be used to obtain curves relating a measure of the seismic response of a structure (displacement at the roof, damage, etc.) to a variable that describes seismic intensity, such as peak ground acceleration (PGA). Several damage indices can be calculated from the dynamic response of a structure (Carr 2002; Kamaris et al. 2013), and are related to a reduction in the capacity of buildings' structural elements. Most of the damage indices proposed to date take values in the range of 0 to 1, where 0 indicates no damage and 1 collapse. Park and Ang (1985), proposed one of the most frequently used seismic damage indices, DI_{PA} , for reinforced concrete buildings, which considers both the maximum structural response and the cyclic load effect (Kostinakis et al. 2015; Vargas et al. 2015). This index also used for steel buildings with results good (Málaga-Chuquitaype and Elghazouli 2012).

¹Research professor, Ph.D., DAIA, Universidad Juárez Autónoma de Tabasco, México, alberto.diaz@ujat.mx

²Ph.D, DECA, Polytechnic University of Catalonia (UPC), Barcelona, Spain, luis.pujades@upc.edu

³Ph.D, DECA, Polytechnic University of Catalonia (UPC). Barcelona, Spain, alex.barbat@upc.edu

⁴Ph.D, DECA, Polytechnic University of Catalonia (UPC). Barcelona, Spain, yeudy.felipe.vargas@upc.edu

⁵Ph.D, DECA, Polytechnic University of Catalonia (UPC). Barcelona, Spain, jose.ramon.gonzalez@upc.edu

⁶M.Sc, DECA, Polytechnic University of Catalonia (UPC). Barcelona, Spain, rodrigo.esteban.alva@upc.edu

Considerable computational effort is required to calculate damage curves based on IDA. To avoid this effort, non-linear static analysis (NLSA) offers an interesting alternative due to its simplicity (Mwafy and Elnashai 2001; Kim and Kurama 2008), but the results must be in good agreement with those provided by IDA. Several researchers have employed NLSA to estimate parameters related to the dynamic response of structures (Fragiadakis and Vamvatsikos 2010; Celarec and Dolšek 2013; Vargas et al. 2013; Pujades et al. 2015; Barbat et al. 2016). In the present article, a new damage index for steel buildings is proposed that can be obtained from the capacity curve. It fits well with the damage index of Park and Ang. The mathematical formulation of the new damage index is based on energy functions and on the idea proposed by Pujades et al. (2015) of using a calibration parameter to determine the contribution to damage of two or more simple functions and, thus, to obtain good agreement with a relatively more complex damage index. A seven-storey steel building under the seismic actions expected in Mexico City was used as the test bed. This case is presented with a probabilistic approach based on the Monte Carlo method and on the Latin hypercube sampling (LHS) technique is also included. The cases studied in this article show that the new damage index for the type of steel structures analysed herein can be used to assess expected damage directly from the capacity curve, in a straightforward way, thus avoiding the considerable computational effort involved in dynamic simulations.

2. THE PROPOSED DAMAGE INDEX

The energy damage index, EDI, proposed is a linear combination of two energy functions: 1) the strain energy, E_{so} , associated with the stiffness variation and the ductility of the structure and 2) the energy dissipated associated to hysteretic cycles, E_D . These functions are based on the formulation of the equivalent viscous damping ratio proposed by Chopra (1995) where two energies can be obtained from the capacity spectrum, E_{so}' and E_D' . These energies are used in the well-known capacity spectrum method (Freeman 1998) and used in the ATC-40 report (1996) and the FEMA-273 report (1997) to obtain the performance point. The energy E_{so} is the maximum strain energy associated with a cycle of motion, that is the area under the secant stiffness of any spectral displacement S_d in the capacity spectrum, $F(S_d)$, which can be calculated as:

$$E_{so}' = \frac{(F(S_d) * S_d)}{2} \quad (1)$$

The energy E_D' is the energy dissipated by the structure in a single cycle of motion (single hysteresis loop). According to Chopra (1995), it can be calculated starting from the bilinear representation of the capacity spectrum, as the area enclosed within a single hysteretic loop equivalent to the area of the parallelogram corresponding to the outline of the bilinear representation. The bilinear representation is defined by 2 points: i) the coordinate of the yielding point (S_{dy} , $F(S_{dy})$), and ii) the coordinate of the ultimate capacity point (S_{du} , $F(S_{du})$). Thus, E_D' can be obtained by the following equation (ATC-40 1996):

$$E_D' = 4(F(S_{dy}) * S_{du} - S_{dy} * F(S_{du})) \quad (2)$$

If E_{so}' and E_D' are calculated from the capacity spectrum as a function of the spectral displacement in an incremental manner, the strain energy function, E_{so} and the energy dissipated by hysteresis function, E_D , are obtained. Combining these functions, the energy damage index, EDI, is derived adopting two following the criteria: i) both functions are normalized to 1 for the value related to the ultimate spectral displacement of the capacity spectrum; ii) both functions will have a value equal to zero within the linear range of the structure because the expected damage in this zone should be zero. Thus, EDI can be calculated through the following equation:

$$EDI = \eta E_{so} + (1 - \eta) E_D \cong DI_{PA} \quad (3)$$

Observe that Park and Ang (1985) index, DI_{PA} , can be used to calibrate the value of parameter η . The parameter η represents the percentage of the contribution to the damage of the function E_{SO} , while $(1-\eta)$ is the percentage of the contribution to the damage of the function E_D . This parameter varies between 0 and 1; it shows that a higher contribution to damage by the strain energy is related to a high value of η and a low value of η indicates that the main contribution to damage is the energy dissipated by hysteresis. The calculation and implementation of EDI are presented in the next section.

3. BUILDING AND SEISMIC ACTIONS USED

3.1 Structural model

A three-storey steel building with four spans is used to illustrate the computation of the proposed energy capacity damage index. This building has been studied extensively by Diaz et al. (2017a) to assess its performance and expected seismic damage under conditions in Mexico City. The main geometric characteristics and structural sections of the building are shown in Figure 1. The structural system of the building is a special moment frame (SMF), composed of beams and columns with W sections (American wide flange section) that are joined by means of prequalified connections (ANSI/AISC 358-10 2010) of a fully restrained (FR) type. This structure was designed as an office building, considering the provisions of NTC-DF (2004) and ANSI/AISC 341-10 (2010). The design of the SMFs satisfies the criterion of strong column-weak beam. Both static and dynamic nonlinear structural analyses were performed using Ruaumoko 2D software (Carr 2002). Beams and columns were modelled as FRAME type members, with plastic hinges at their ends. The plastic hinges follow the bi-linear hysteresis rule. The hardening and strength reduction were calculated, based on the ductility factor (see Appendix A - Ruaumoko 2D (Carr 2002)). Due to limitations of the adopted model, which only reproduces the failure by bending moment, the interaction between the bending moment and the axial force has not been considered. Obviously, most of the damage of this type of building is expected to occur at the ends of the elements, mainly because the effects of the bending moment. The values of strength and ductility were calculated according to the modified Ibarra–Medina–Krawinkler (IMK) model (Ibarra et al. 2005; Lignos and Krawinkler 2011, 2013). The panel zones were modelled using the rotational stiffness in connections, according to the model of Krawinkler (1978) included in FEMA 355C (2000). For the damping, the Rayleigh model is assumed and a damping ratio of 2% (SAC 1995; PEER/ATC 72-1 2010). The fundamental period, T_1 , of the building model is 0.63 s.

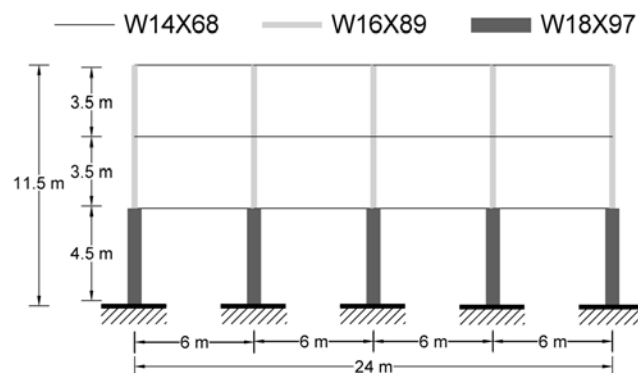


Figure 1. Geometry and structural section of the archetype building.

3.2 Seismic actions

Damage curves must be obtained using the IDA method to calibrate the new damage index, EDI. Acceleration records of Mexico City were used in this example. The design spectrum for the IIIa

seismic area, according to NTC-DF (2004), was taken as a target spectrum. The selection method proposed by Vargas et al. (2013) was applied to a database containing 2554 accelerograms recorded in the Mexico City area (Diaz et al. 2015). Four accelerograms were thus selected whose mean response spectra are compatible with the target spectrum. The main characteristics of these accelerograms are shown in Table 1.

Table 1. Characteristic of the seed accelerograms used in seismic zone IIIa in Mexico City.

Acc.	Station	Date	Duration (s)	Epicentre			Magnitude (Mw)	Component	PGA (cm/s ²)	Epicentral distance (km)	Azimut Sta-Epi
				Latitude	Longitude	Depth (km)					
1	AL01	18/04/2014	165.77	17.18 N	101.19 W	10	7.2	S00E	28.86	330.89	221.04
2	HJ72	18/04/2014	167.47	17.18 N	101.19 W	10	7.2	N90W	32.19	331.06	221.39
3	MJSE	15/06/1999	144.01	18.18 N	97.51 W	69	7.0	N76W	13.76	222.31	128.79
4	TL55	30/09/1999	173.86	15.95 N	97.03 W	16	5.2	N90E	15.62	447.59	149.67

Each one of the accelerograms in Table 1 was used as a seed within a probabilistic spectral matching technique (Hancock et al. 2006; Diaz et al. 2017a) to obtain 5 new accelerograms whose response spectra show good agreement with the target spectra. Thus, a set of 20 matched accelerograms was obtained, which were considered suitable to deal with uncertainties in the seismic actions, to validate the proposed damage index in a probabilistic environment. Figure 2a shows the seed accelerogram 1 and one of the matched accelerograms that was used to perform the IDA analysis. Figure 2b shows the target spectrum, the response spectrum of seed accelerogram 1 and the response spectrum of the matched accelerogram.

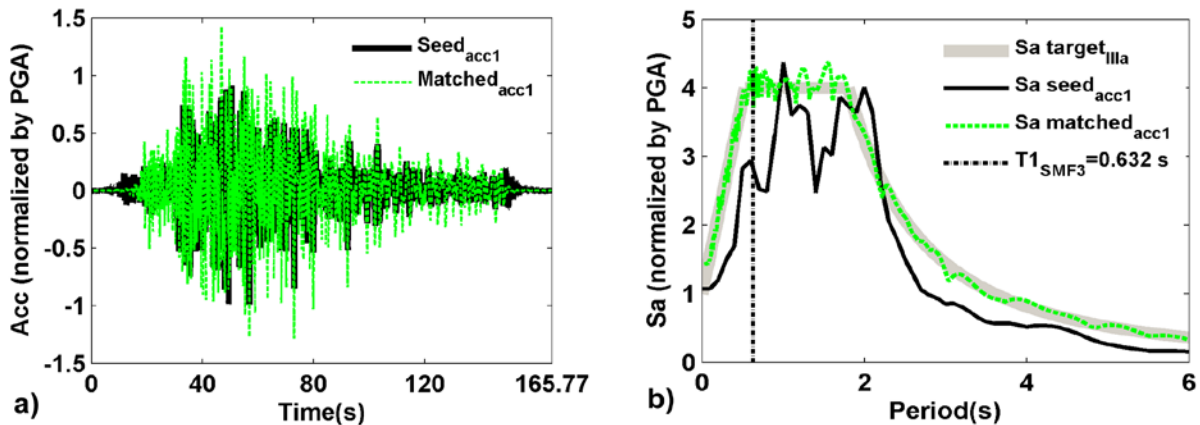


Figure 2. a) The seed accelerogram 1 and the matched accelerogram, and b) the target spectrum (IIIa) and the response spectra for seed accelerogram 1 and the matched accelerogram.

4. EXAMPLE OF IMPLEMENTATION THE NEW DAMAGE INDEX

4.1 Capacity curve

The capacity curve was obtained by means of an adaptive pushover analysis (PA), implemented in Ruaumoko software (Carr 2002). This method is independent of the initial loading pattern, as it adapts the pattern at each step of the PA, according to the shape of the first vibration mode of the structure. The ultimate capacity is established when one of the following criteria is fulfilled: i) ω^2 is less than $10^{-6} \omega^2$ at the first step, where ω is the tangent fundamental natural frequency in the Modified Rayleigh Method; ii) the Newton Raphson iteration is not achieved within a maximum number of specified cycles; iii) the stiffness matrix becomes singular; and iv) a specified maximum structure displacement is reached. In the NLSAs of the studied models, many cycles of the Newton Raphson method were

considered. Moreover, a large maximum limit for structure displacement was considered. Thus, the failure criteria are expected to be related to criteria i or iii. The conventional pushover analysis and the adaptive pushover analysis, P_{ad} , for buildings with structural response dominated by their fundamental mode provide similar capacity curves; however, in this research, the P_{ad} was preferred, because it includes predefined criteria to determine the ultimate capacity point. This aspect is useful in probabilistic assessments to define the collapse for each analysis. Moreover, these failure criteria, predefined in the capacity curve, allow improving compatibility with the ultimate capacity achieved in the IDA. However, conventional pushover can be also used if the ultimate capacity point is adequately defined. Figure 3a shows the capacity curve that was obtained.

4.2 Incremental dynamic analysis.

Incremental dynamic analysis was performed for the building using the matched accelerogram shown in Figure 2a. The PGA of the record was increased until the collapse of the structure, established in terms of ultimate displacement δ_u . In this case, the collapse displacement of the building corresponds to a PGA of 1 g. The DI_{PA} function of the roof displacement, δ , for the building is shown in Figure 3. The capacity curve and the DI_{PA} were used in subsequent sections to calibrate the new damage index.

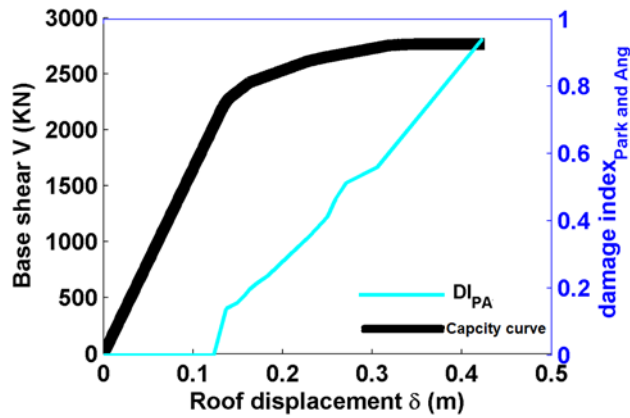


Figure 3. Capacity curve and the DI_{PA} by IDA of the building.

4.3 Energy damage index for the building.

To calibrate the simplified energy damage index EDI, it was considered that the evolution of damage DI_{PA} is closely related to the roof displacement caused by the seismic action. These displacements are expected to differ for different seismic actions, because important properties such as the duration and frequency content of each seismic action may vary, causing a different structural response for equal PGA values.

The IDA method provides the displacement pattern as a function of the PGA. Otherwise, in NLSA, the performance point for each PGA value must be calculated in order to define the roof displacements as a function of the increased PGA of seismic action, $S_{dpp}(PGA)$. In the present research, the energy balance (EB) method (Mezzi et al. 2006; Leelataviwat et al. 2009) was used to obtain displacement patterns due to seismic actions. The EB method is based on the relation between the energy response spectrum of the accelerogram (S_{aE}) and the capacity curve, converted to Energy Accumulated by Deformation (EAD). Both curves must be expressed in spectral - energy displacement ($S_d - E$) normalized by the energy at the yielding point of the capacity curve (E_y). The energy response spectrum S_{aE} is obtained with the equations proposed by Chopra and Goel (2002); while the EAD curve is defined as the area under the capacity spectrum $F(\xi)$, with the following equation:

$$EAD(S_d) = \int_0^{S_d} F(\xi) d\xi \quad 0 \leq \xi \leq S_u; \quad 0 \leq EAD(S_d) \leq EAD(S_d) \quad (4)$$

Further details of these energy functions and how the demand-capacity point is calculated are described in the research by Leelataviwat *et al.* (2009) and Diaz *et al.* (2017b).

Static roof displacements were then determined by assuring the energy balance, considering the PGA incrementally and converting the $Sd_{pp}(PGA)$ into roof displacements, $\delta(PGA)$. The energy functions E_{so} and E_D are obtained based on the static roof displacement function. The DI_{PA} of the building is used to calibrate the energy capacity damage index to obtain $\eta=0.70$. This means that the contribution to the damage index of the strain energy function, E_{so} , is 70%, while the contribution of the hysteretic dissipated energy, E_D , is 30%. These percentages would vary for different seismic actions.

Figure 4a shows the E_{so} , E_D , EDI and DI_{PA} for the building. Both indices show very good agreement. Observe that the damage curves that were calculated can be also related to the PGA by considering the $\delta(PGA)$. Thus, the proposed energy damage index can be directly related to an intensity measure of the earthquake. Figure 4b shows $E_{so}(PGA)$ and $E_D(PGA)$, $DI_{PA}(PGA)$ and EDI(PGA) functions. In the case studied here, the EDI(PGA) also shows very good agreement with $DI_{PA}(PGA)$.

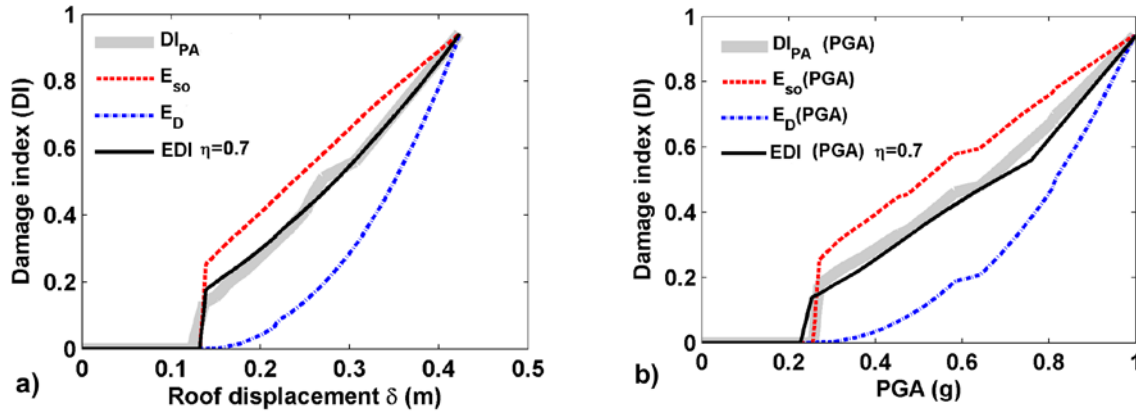


Figure 4. a) DI_{PA} and EDI; and b) $DI_{PA}(PGA)$ and EDI(PGA) of the building.

5. PROBABILISTIC APPROACH

The model of the studied building was then used to estimate the new damage index from a probabilistic perspective. It was proved that the proposed damage index fits well the results obtained with the IDA, even when several uncertainties were considered in the mechanical properties of the materials and the seismic action. For the probabilistic approach, the Monte Carlo method (Rubinstein 1981; Hurtado and Barbat 1998) and the Latin hypercube sampling (LHS) technique (McKay *et al.* 1979; Iman 1999; Vamvatsikos 2014) were used to optimize the number of samples. The strength and ductility of the beams and columns were considered random variables in the modified Ibarra–Medina–Krawinkler (IMK) model (Ibarra *et al.* 2005; Lignos and Krawinkler 2011, 2013). The backbone curve of the modified IMK model was defined by three strength parameters (M_y = effective yield moment; M_c = capping moment strength or post-yield strength ratio M_c/M_y and $M_r = \kappa \cdot M$, residual moment) and by four deformation parameters: θ_y = yield rotation; θ_p = pre-capping plastic rotation for monotonic loading (difference between yield rotation and rotation at the maximum moment); θ_{pc} = post-capping plastic rotation (difference between rotation at maximum moment and rotation at complete loss of strength); and θ_u = ultimate rotation capacity (see Figure 5a). The strength parameters can be determined for W sections according to Lignos and Krawinkler (2011, 2013) and from the recommendations of PEER/ATC 72-1(2010) using the following equations:

$$M_y = 1.17 \cdot Z \cdot f_y \quad (5)$$

$$M_c = 1.11 \cdot M_y \quad (6)$$

$$M_r = 0.4 \cdot M_y \quad (7)$$

The deformation parameters can be determined for W sections by means of the following multi-variable empirical equations that were developed by Lignos and Krawinkler (2011, 2013) and included in the PEER/ATC 72-1(2010).

$$\theta_y = (M_y/k_o)/L = (M_y/6 \cdot E \cdot I)/L \quad (8)$$

$$\theta_p = 0.0865 \cdot \left(\frac{h}{t_w}\right)^{-0.365} \cdot \left(\frac{b_f}{2 \cdot t_f}\right)^{-0.140} \cdot \left(\frac{L}{d}\right)^{0.340} \cdot \left(\frac{c_{unit}^1 \cdot d}{533}\right)^{-0.721} \cdot \left(\frac{c_{unit}^2 \cdot f_y}{355}\right)^{-0.721} \quad \sigma_{In}=0.32 \quad (9)$$

$$\theta_{pc} = 5.63 \cdot \left(\frac{h}{t_w}\right)^{-0.565} \cdot \left(\frac{b_f}{2 \cdot t_f}\right)^{-0.800} \cdot \left(\frac{c_{unit}^1 \cdot d}{533}\right)^{-0.280} \cdot \left(\frac{c_{unit}^2 \cdot f_y}{355}\right)^{-0.430} \quad \sigma_{In}=0.25 \quad (10)$$

$$\theta_u = 1.5 \cdot (\theta_y + \theta_p) \quad (11)$$

In these equations, k_o is the initial elastic stiffness; I is the inertia moment; c_{unit}^1 and c_{unit}^2 are coefficients for units conversion; h/t_w is the ratio between the web depth and the thickness; L/d is the ratio between the span and the depth of the beam; $b_f/(2 \cdot t_f)$ is the width/thickness ratio of the beam flange; and σ_{In} is the standard deviation, assuming a lognormal fit of experimental data.

In this research, the modified IMK model of the structural sections was defined by all the strength parameters based on the expected yield strength, f_y ; and the deformation parameters (ductility) based on θ_p and θ_{pc} . PEER/ATC 72-1 (2010) recommends that, when experimental results of cyclic degradation of stiffness in the structural elements are not available, as in this study, the parameters θ_p and θ_{pc} should be adapted as follows: $\theta'_p=0.7\theta_p$ and $\theta'_{pc}=0.5\theta_{pc}$. Figure 5a shows the model used herein based on the parameters of the modified IMK model, and the bi-linear hysteresis rule with strength reduction based on the ductility as defined in Ruaumoko.

For a better representation of physical randomness in the problem, for each structural element, a random sample of the three parameters (f_y , θ_p and θ_{pc}) was generated. Then, the properties of strength and ductility of the plastic hinges of each element were estimated. It was assumed that the hinges at both ends of the elements were the same. Thus, the 3-storey model with 27 elements (15 columns and 12 beams) had 81 random variables. Table 2 shows the mean value μ , the standard deviation, the coefficient of variation (COV) and the assumed probability distributions of these 3 parameters.

Moreover, to avoid unrealistic samples in LHS simulations, the normal distribution of f_y and lognormal distributions of θ_p and θ_{pc} were truncated at both ends. The lower and upper limits were determined by the mean value ± 2 standard deviations ($\mu \pm 2\sigma$). The purpose of this truncation was to avoid under- or overestimates of the capabilities of the elements with samples without physical meaning.

Table 2. Probabilistic property of strength and ductility random variables.

Structural section	Type	Variable	Mean (μ)	Standard deviation (σ or σ_{In})	Function
W14X68	Strength	f_y	375.76 MPa*	26.68 MPa (COV=0.071*)	Normal distribution
	Ductility	θ_p	0.054 rad*	$\sigma_{In}=0.32^*$	Lognormal distribution
	Ductility	θ_{pc}	0.188 rad*	$\sigma_{In}=0.25^*$	Lognormal distribution
W16X89	Strength	f_y	375.76 MPa*	26.68 MPa (COV=0.071*)	Normal distribution
	Ductility	θ_p	0.047 rad*	$\sigma_{In}=0.32^*$	Lognormal distribution
	Ductility	θ_{pc}	0.210 rad*	$\sigma_{In}=0.25^*$	Lognormal distribution
W18X97	Strength	f_y	375.76 MPa*	26.68 MPa (COV=0.071*)	Normal distribution
	Ductility	θ_p	0.044 rad*	$\sigma_{In}=0.32^*$	Lognormal distribution
	Ductility	θ_{pc}	0.183 rad*	$\sigma_{In}=0.25^*$	Lognormal distribution

* Based on the report by Lignos & Krawinkler (2011) for statistics of material yielding strength, obtained from flanges-webs tests for A572 grade steel.

* For the steel, structural W sections were determined by means of the multi-variable empirical Equations (9) and (10).

Another important sampling issue is the correlation among variables. Two types of correlations were considered in this research: intra- and inter-element. The intra-element correlation was given by the relation among the three parameters simulated for the same hinge; these correlations can be derived

from Eqs. (9) and (10) (Lignos and Krawinkler 2011, 2013) and are defined in Table 3. The inter-element was defined based on research conducted by Idota et al. (2009) and Kazantzi et al. (2014) on consistency in workmanship and material quality between different steel structural W sections. An inter-element correlation of 0.65 was used herein for the same section type, and a null correlation was assumed for different sections.

Table 3. Intra-element correlation for random variables of beams and columns.

	f_y	θ_p	θ_{pc}
f_y	1	0	0
θ_p	0	1	0.69
θ_{pc}	0	0.69	1

In order to assess the seismic behaviour of the building in a probabilistic environment, 200 NLSAs and 200 NLDAs were performed using the same structural models for both the static and dynamic analysis. Figure 5b shows an example of the modified IMK model used in the 12-beam W14x68 section of the probabilistic models.

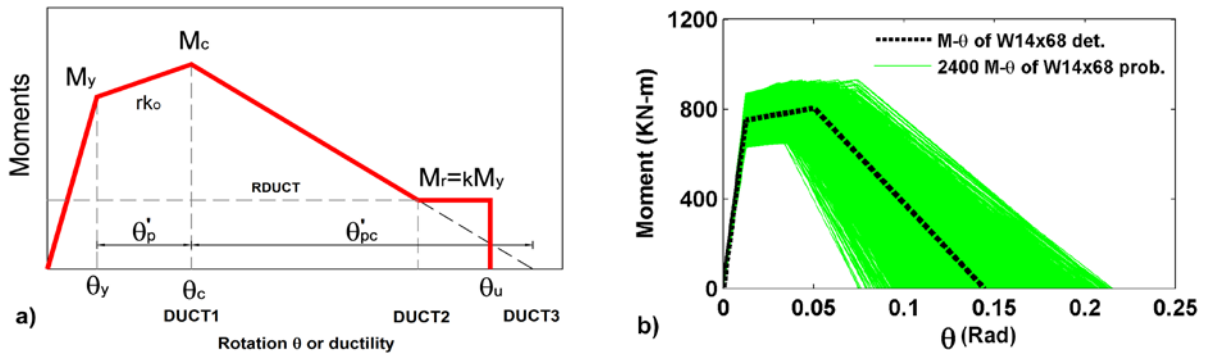


Figure 5. a) Modified IMK model: monotonic curve; b) an example of the modified IMK model used in the structural section (W14x68) of the probabilistic models.

Seismic action was also considered in a probabilistic way using the set of 20 matched accelerograms developed in Section 3.2 and their corresponding response spectra shown in Figure 6. The mean of the 20 response spectra accurately represents the target spectrum of the study area (Mexico City). Figure 6 also shows the fundamental period variation of the probabilistic models, $T1_{SMF3}$ prob. For each of the probabilistic IDA, one of the 20 available records was randomly selected, using a uniform probability distribution.

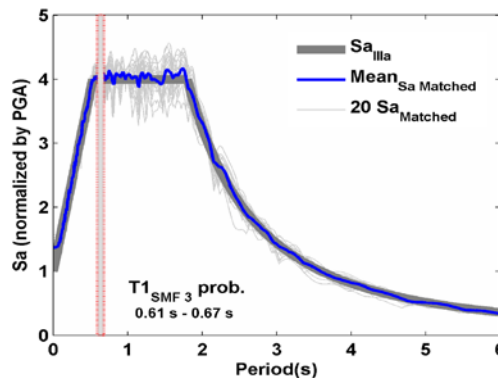


Figure 6. Response spectra of the 20 matched accelerograms and the mean spectrum. The fundamental periods of the probabilistic models are also depicted.

Figure 7a shows the probabilistic capacity curves obtained using the procedure explained in Section 4.1, and the curve representing the 50th percentile (median) of the curves. Figure 7b shows the probabilistic DI_{PA} and Figure 8b the probabilistic $DI_{PA}(PGA)$, both obtained with IDA analysis, in

accordance with the procedure explained in Section 4.2. Their respective 50th percentiles (medians) are also depicted.

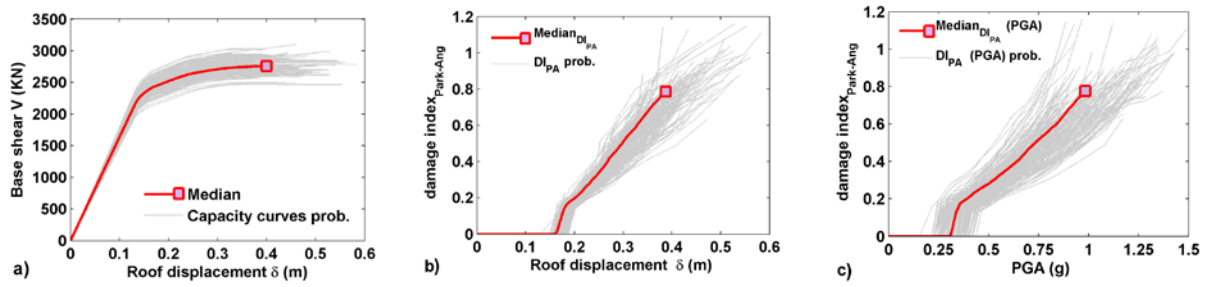


Figure 7. a) Probabilistic capacity curves; b) the DI_{PA} probabilistic and c) the DI_{PA} (PGA) probabilistic.

The static displacement function of each probabilistic model was determined based on the energy balance between its ADE curve and the response spectrum in EDRS format of the matched accelerogram that was used in the IDA in the same probabilistic model.

Then, the energy capacity damage index, EDI, was calculated and calibrated with the corresponding DI_{PA} . Figure 8a shows the curves that were obtained. In this figure, the DI_{PA} curves calculated via IDA are shown together with the corresponding EDI curves. The median curves are also shown in Figure 8a. The median EDI curve shows a good fit with the median DI_{PA} curve for parameter $\eta=0.62$. Therefore, for probabilistic cases, the contribution to the EDI of the strain energy function, E_{so} , is 62%, while the contribution of the energy dissipated by hysteretic cycles, E_D , is 38%. The EDI can be well fitted to the DI_{PA} . Figure 8b shows the $DI_{PA}(PGA)$ and the EDI(PGA) probabilistic functions. Again, in all cases, the agreement was very good, especially in the median value. Therefore, the new damage index can also be used to establish the expected damage in function of the intensity of the seismic action.

Finally, parameter η is crucial in the energy damage index. Note that each DI_{PA} curve is obtained for a specific seismic action. Different seismic actions can be expected to lead to different Park and Ang index values and, therefore, to different values of the parameter η . Thus, parameter η allows the new index, EDI, to fit the response and the expected damage properly when the building is subjected to different seismic actions.

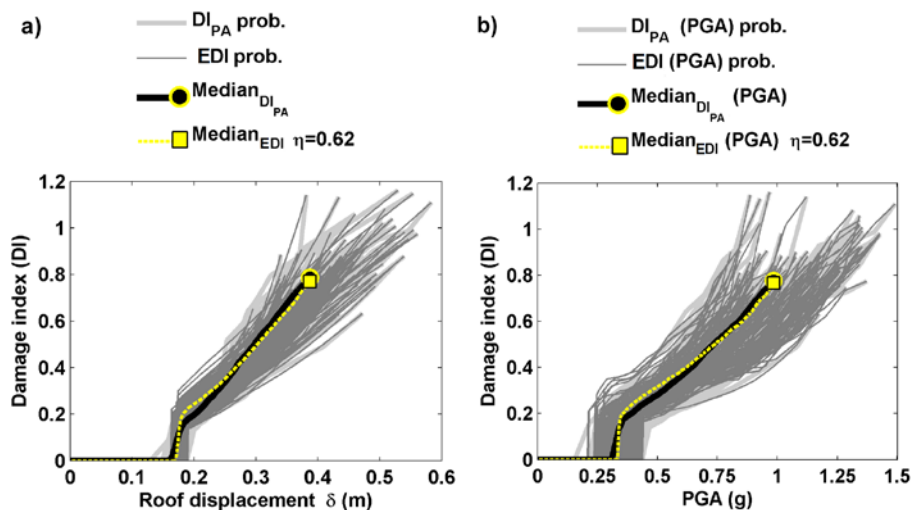


Figure 8. a) DI_{PA} and EDI probabilistic curves, and b) $DI_{PA}(PGA)$ and EDI(PGA) probabilistic curves.

6. CONCLUSIONS

In this paper, a new damage index was developed, based on the capacity curve obtained by nonlinear static analysis. Two energy functions were defined. The former is strain energy, E_{so} , which is associated with stiffness variation and the ductility of the structure. The latter is the energy dissipated by damping, E_D , which is related to the energy dissipated by hysteretic cycles. Using a linear combination of these two energy functions by means of a parameter of contribution to damage η , the new damage index, EDI, was defined. Parameter η was calibrated using the well-known Park and Ang damage index, DI_{PA} , which is obtained from IDA. Both damage indices show good agreement.

Concerning the damage index for the buildings and the seismic actions studied in this research, on average, the Park and Ang damage index is well fitted by the combination of 62% of the E_{so} function and 38% of the E_D function.

The energy balance method that was applied incrementally determined the static displacement pattern in the studied building under the applied seismic actions. EDI can be expressed in terms of the increase of PGA, $EDI(PGA)$. The advantage of $EDI(PGA)$ is that it provides a scenario of expected damage, based on the characteristics of the seismic action to which the building is subjected. This result is similar to the damage scenario obtained with IDA.

The distribution parameter, η , depends on the characteristics of the seismic action. That is, it can be expected that different seismic actions lead to different DI_{PA} and, therefore, to different values of the parameter η . The relation between the parameter η and the type of frame for different buildings can be also studied.

It is clear that if the new damage index needs to be calibrated for each new building and for each different seismic action, the advantages of this simplified damage index vanish. Anyhow, ongoing research shows that values of parameter η are very stable. Values in the range 0.6-0.7 are obtained. Values in the low part of the range (around 0.6) are obtained for long duration seismic actions. On the contrary, high values (around 0.7) are obtained for impulsive near-fault short accelerograms. Therefore, accurate calibrations of this parameter η , can lead to tabulated values for different seismic actions and building types.

Because the new damage index is calibrated so that it is equivalent to the Park and Ang damage index, it does not improve the quantitative damage assessment but, if tabulated values of the parameter η are available, the new damage index can be used in a quick, straightforward and routine way.

The most important contribution of this article is that the new damage index based on two energy functions can be obtained directly from the capacity curves in a straightforward way, and provides adequate results for assessing expected damage in buildings, as a function of the characteristics of the applied seismic action, such as for instance, the frequency content and duration. Therefore, it can be a useful tool to evaluate the seismic damage of buildings, especially in a probabilistic environment in which computational times can be significantly reduced.

7. ACKNOWLEDGEMENTS

This research was partially funded by the Ministry of Economy and Competitiveness (MINECO) of the Spanish Government and by the European Regional Development Fund (ERDF) of the European Union (EU) through projects referenced as: CGL2011-23621 and CGL2015-65913-P (MINECO/FEDER, UE).

8. REFERENCES

AISC 341-10 (2010) Seismic Provisions for Structural Steel Buildings. American Institute of Steel Construction.

ANSI/AISC 358 (2010) Prequalified connections for special and intermediate steel moment frames for seismic applications. American Institute of Steel Construction.

ATC 40 (1996) Seismic evaluation and retrofit of concrete buildings. Applied Technology Council. Redwood City, California.

- Barbat AH, Vargas YF, Pujades LG, Hurtado JE (2016) Evaluación probabilista del riesgo sísmico de estructuras con base en la degradación de rigidez. *Rev. int. métodos numér. cálc. diseño ing.* 32(1):39–47.
- Carr AJ (2002) Ruauumoko–inelastic dynamic analysis program. Department of Civil Engineering, University of Canterbury, Christchurch.
- Celarec D, Dolšek M (2013) The impact of modelling uncertainties on the seismic performance assessment of reinforced concrete frame buildings. *Engineering Structures.* 52(1): 340-354
- Chopra AK, Goel RK. (2002) A modal pushover analysis procedure for estimating seismic demands for buildings. *Earthq Eng Struct Dyn.* 31(3):561-582.
- Chopra AK. (1995) *Dynamics of structures: theory and applications to earthquake.* Chaps. 3. Englewood Cliffs, New Jersey: Prentice Hall, p. 944.
- Diaz SA, Pujades LG, Barbat AH, Hidalgo-Leiva DA, Vargas-Alzate YF (2017a) Capacity, damage and fragility models for steel buildings. A probabilistic approach. *Bull Earthq Eng.* <https://doi.org/10.1007/s10518-017-0237-0>.
- Diaz SA, Pujades LG, Barbat AH, Vargas-Alzate YF, Hidalgo-Leiva DA (2017b) Energy damage index based on capacity and response spectra. *Eng Struct.* 152(1):424-436. <https://doi.org/10.1016/j.engstruct.2017.09.019>
- Diaz SA, Pujades LG, Barbat AH, Félix JL (2015) Efecto de la direccionalidad en la amenaza sísmica de la Ciudad de México. In: 20 th Congreso Nacional de Ingeniería Sísmica. México. Acapulco, Guerrero. ISSN: 2448-5721.
- FEMA 273 (1997) NEHRP guidelines for the seismic rehabilitation of buildings, FEMA 273; and NEHRP commentary on the guidelines for the seismic rehabilitation of buildings, FEMA 274. Washington, D.C.: Federal Emergency Management Agency. 1997; p. 435.
- FEMA 355C (2000) State of the art report on system performance of steel moment frames subject to earthquake ground shaking. SAC Joint Venture Partnership for the Federal Emergency Management Agency. Washington, D.C.
- Fragiadakis M, Vamvatsikos D (2010) Fast performance uncertainty estimation via pushover and approximate IDA. *Earthq Eng Struct Dyn,* 39: 683-703.
- Freeman SA (1998) The capacity spectrum method as a tool for seismic design. In: *Proceedings of the 11th European conference on earthquake engineering.* Paris, France.
- Hancock J, Watson-Lamprey J, Abrahamson N, Bommer J, Markatis A, McCoy E, Mendis R, (2006) An improved method of matching response spectra of recorded earthquake ground motion using wavelets, *Journal of Earthquake Engineering,* 10(Special Issue 1): 67-89.
- Hurtado JE, Barbat AH. Monte Carlo Techniques. In *Computational Stochastic Mechanics.* Arch Comput Methods Eng. 1998; 5(1):3–29.
- Ibarra LF, Medina RA, Krawinkler H (2005) Hysteretic models that incorporate strength and stiffness deterioration. *Earthq Eng Struct Dyn* 34 (12):1489–1511.
- Idota H, Guan L, Yamazaki K (2009) Statistical correlation of steel members for system reliability analysis. In: *Proceedings of the 9th international conference on structural safety and reliability (ICOSSAR).* Osaka, Japan.
- Iman RL (1999). Appendix A: Latin Hypercube Sampling. *Encyclopedia of Statistical Sciences,* Update Volume 3, Wiley, NY. 408-411.
- Kamaris GS, Hatzigeorgiou GD, Beskos DE (2013) A new damage index for plane steel frames exhibiting strength and stiffness degradation under seismic motion. *Eng Struct* 46:727-736.
- Kazantzi AK, Vamvatsikos D, Lignos DG (2014) Seismic performance of a steel moment-resisting frame subject to strength and ductility uncertainty. *Eng Struct* 78:69–77.

- Kim S-P, Kurama YC (2008) An alternative pushover analysis procedure to estimate seismic displacement demands. *Eng Struct* 30(12):3793–3807.
- Kostinakis K, Athanatopoulou A, Morfidis K. (2015) Correlation between ground motion intensity measures and seismic damage of 3D R/C buildings. *Eng. Struct.* 82:151–167.
- Krawinkler H (1978) Shear in beam-column joints in seismic design of steel frames. *Eng J* 15(3):82–91.
- Leelataviwat S, Saewon W, Goel SC. (2009) Application of energy balance concept in seismic evaluation of structures. *J. Struct. Eng. ASCE.* 135(2):113-121.
- Lignos DG, Krawinkler H (2013) Development and utilization of structural component databases for performance-based earthquake engineering. *J Struct Eng* 139(8):1382–1394.
- Lignos DG, Krawinkler H (2011) Deterioration modeling of steel components in support of collapse prediction of steel moment frames under earthquake loading. *J Struct Eng* 137(11):1291-1302.
- Málaga-Chuquitaype C, Elghazouli AY. (2012) Evaluation of fatigue and Park and Ang damage indexes in steel structures. In: *Proc. 15thWorld Conf. Earthq. Eng.* Lisbon Portugal.
- McKay MD, Conover WJ, Beckman R. (1979). A comparison of three methods for selecting values of input variables in the analysis of output from a computer code. *J. Technometrics.* 1979; 21(2):239–245.
- Mezzi M, Comodini F, Lucarelli M, Parducci A, Tomassoli E. (2006) Pseudo-energy response spectra for the evaluation of the seismic response from pushover analysis. In: *Proc. First European Conference on Earthquake Engineering and Seismology, Switzerland.* 2006; paper number 1183.
- Mwafy A, Elnashai A (2001) Static pushover versus dynamic collapse analysis of RC buildings. *Eng Struct* 23(5):407–424.
- NTC-DF (2004): Norma técnica complementaria del Distrito Federal. Technical Report Gaceta oficial del Distrito Federal, México.
- Park Y-J, Ang AH-S (1985) Mechanistic seismic damage model for reinforced concrete. *ASCE J Struct Eng ASCE* 111:722-739.
- PEER/ATC 72-1 (2010) Modeling and acceptance criteria for seismic design and analysis of tall buildings. Applied Technology Council and Pacific Earthquake Engineering Research Center.
- Pujades LG, Vargas-Alzate YF, Barbat AH, González-Drigo JR. (2015) Parametric model for capacity curves. *Bull. Earthq. Eng.* 13(5):1347–1376.
- Rubinstein RY. *Simulation and the Monte Carlo method*, John Wiley. New York. 1981; p. 372.
- SAC (1996) Analytical and field investigations of buildings affected by the Northridge earthquake. Report No. SAC-95-04, prepared by SAC Joint Venture, a partnership of SEAOC, ATC and CUREE.
- Vamvatsikos D (2014) Seismic performance uncertainty estimation via IDA with progressive accelerogram-wise latin hypercube sampling. *J. Struct. Eng.*, 2014, 140(8): A4014015-1-10.
- Vamvatsikos D, Cornell CA (2002) Incremental dynamic analysis. *Earthq Eng Struct Dyn* 31 (3):491–514.
- Vargas YF, Pujades LG, Barbat AH, Hurtado JE (2013) Capacity, fragility and damage in reinforced concrete buildings: A probabilistic approach. *Bull Earthq Eng* 11(6):2007–2032.
- Vargas YF, Pujades LG, Barbat AH, Hurtado JE. Probabilistic seismic damage assessment of RC buildings based on nonlinear dynamic analysis. *The Open Civil Engineering Journal.* 2015; 9(Suppl. 1, M 12): 344-350.